GIANT PLANET IONOSPHERES AND THERMOSPHERES: THE IMPORTANCE OF ION-NEUTRAL COUPLING

STEVE MILLER, ALAN AYLWARD and GEORGE MILLWARD
Atmospheric Physics Laboratory, Department of Physics and Astronomy, University College London, London WC1E 6BT, U.K.

Received: 15 April 2004; Accepted in final form: 11 July 2004

Abstract. Planetary upper atmospheres – coexisting thermospheres and ionospheres – form an important boundary between the planet itself and interplanetary space. The solar wind and radiation from the Sun may react with the upper atmosphere directly, as in the case of Venus. If the planet has a magnetic field, however, such interactions are mediated by the magnetosphere, as in the case of the Earth. All of the Solar System's giant planets have magnetic fields of various strengths, and interactions with their space environments are thus mediated by their respective magnetospheres. This article concentrates on the consequences of magnetosphere-atmosphere interactions for the physical conditions of the thermosphere and ionosphere. In particular, we wish to highlight important new considerations concerning the energy balance in the upper atmosphere of Jupiter and Saturn, and the role that coupling between the ionosphere and thermosphere may play in establishing and regulating energy flows and temperatures there. This article also compares the auroral activity of Earth, Jupiter, Saturn and Uranus. The Earth's behaviour is controlled, externally, by the solar wind. But Jupiter's is determined by the co-rotation or otherwise of the equatorial plasmasheet, which is internal to the planet's magnetosphere. Despite being rapid rotators, like Jupiter, Saturn and Uranus appear to have auroral emissions that are mainly under solar (wind) control. For Jupiter and Saturn, it is shown that Joule heating and "frictional" effects, due to ion-neutral coupling can produce large amounts of energy that may account for their high exospheric temperatures.

Keywords: giant planets, ionosphere, thermosphere, ion-neutral coupling

1. Introduction

Although typically less than one part in a million of the mass of a planet's atmosphere is represented by the uppermost layers – the coexisting thermosphere and ionosphere – they form an important boundary between the planet itself and interplanetary space. The solar wind and radiation from the Sun may react with the upper atmosphere directly, as in the case of Venus. If the planet has a magnetic field, however, such interactions are mediated by the magnetosphere, as in the case of the Earth. All of the Solar System's giant planets have magnetic fields of various strengths, and interactions with their space environments are thus mediated by their respective magnetospheres.

The neutral thermosphere absorbs solar extreme ultraviolet (EUV) radiation and is subject to a flux of precipitating particles. These precipitating particles may come directly from the solar wind, if the planet is unmagnetised, or be accelerated by

Space Science Reviews 116: 319–343, 2005.
DOI: 10.1007/s11214-005-1960-4

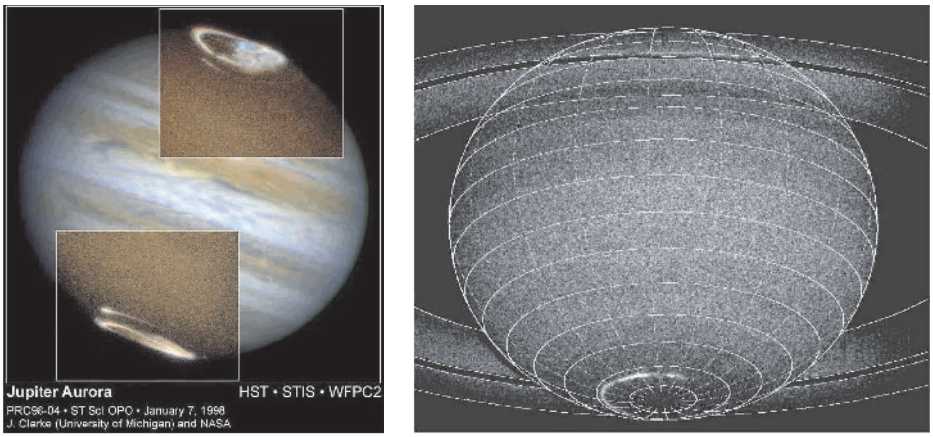

Figure 1. (a) UV images of Jupiter's aurorae superimposed on an optical image of the planet (courtesy J. Clarke, University of Michigan). (b) UV image of Saturn's southern aurora (from Cowley *et al.*, 2004).

fields generated in the magnetosphere, if there is one. Both the absorption of EUV radiation and particle precipitation can cause dissociation and ionisation of the main thermospheric species, and subsequent chemistry can modify the resulting atmospheric composition. The ionosphere refers to that part of the atmosphere where there is a significant proportion of ions and electrons, enough to affect the propagation of radio waves.

Recent work imaging the upper atmospheres of Jupiter, Saturn and Uranus in ultraviolet (e.g. Gérard *et al.*, 1995; Ballester *et al.*, 1998; Clarke *et al.*, 1998; Prangé *et al.*, 1998; Trauger *et al.*, 1998; Vincent *et al.*, 2000; Pallier and Prangé, 2001; Pryor *et al.*, 2001; Waite *et al.*, 2001; Grodent *et al.*, 2003), visible (Vasavada *et al.*, 1999) and infrared (e.g. Satoh *et al.*, 1996; Lam *et al.*, 1997a; Satoh and Connerney, 1999; Trafton *et al.*, 1999) radiation has shown that emission from neutral and ionised species is an important way of tracing the location of energy inputs into the upper atmospheres (Figures 1-2). For the purposes of this chapter, an approximate definition of "auroral emission" is "atmospheric emission in response to particle precipitation" (although this does not cover everything that may be called "auroral"). Thus auroral emission is generally linked to the injection into the atmosphere of particles capable of exciting and ionising atmospheric species. An extensive review of the auroral emissions of all four giant planets is given by Bhardwaj and Gladstone (2000).

Particular progress has been made in understanding how the jovian magnetosphere, and the particle fluxes it produces, map onto the upper atmosphere (Kivelson *et al.*, 1997; Cowley and Bunce, 2001; Hill, 2001; Southwood and Kivelson, 2001). As well as the major magnetospheric signatures, it has even been possible to detect emission due to the perturbations caused by orbiting moons (Connerney *et al.*, 1993; Clarke *et al.*, 1998; Prangé *et al.*, 1998; Clarke *et al.*, 2002). It has

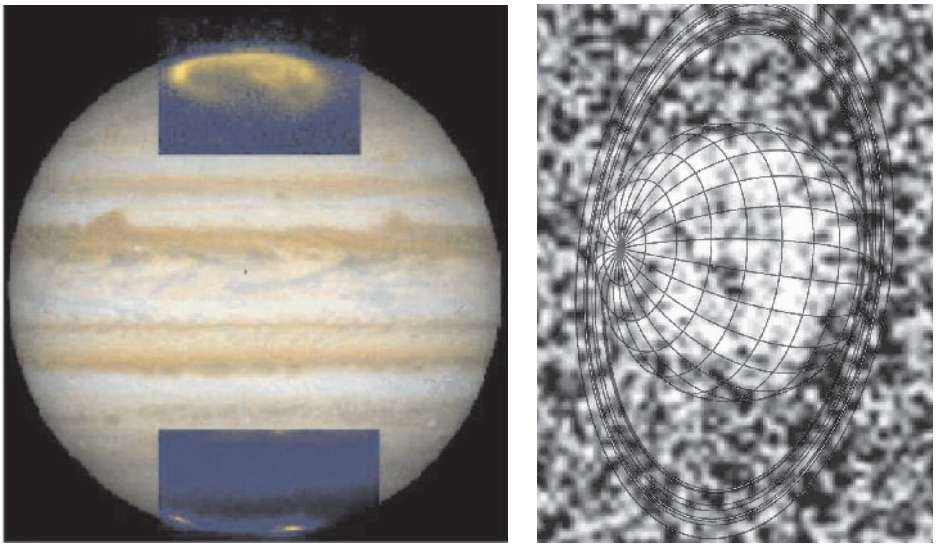

Figure 2. (a) IR images of Jupiter's aurorae taken at 3.953 μm (sensitive to H_3^+ emission) superimposed on an optical image of the planet (courtesy N. Achileos, UCL). (b) IR image of Uranus taken at 3.953 μm (Trafton, Miller and Stallard, unpublished data).

been especially fruitful to link in situ spacecraft measurements of magnetospheric fields and particles to atmospheric emissions. This has led to some referring to the upper atmosphere as a "television screen" for viewing magnetospheric processes.

While not downplaying the importance of this "viewing facility", this article concentrates on the consequences of magnetosphere-atmosphere interactions for the physical conditions of the thermosphere and ionosphere. In particular, we wish to highlight important new considerations concerning the energy balance in the upper atmosphere and the role that coupling between the ionosphere and thermosphere may play in establishing and regulating energy flows and temperatures there. Given the emphasis of this volume on the Cassini/Huygens mission, we will also concentrate on drawing comparisons between Saturn and Jupiter, although other worthwhile comparisons will also be highlighted. In the next two sections, we look at some basic features of the upper atmosphere that will be useful for putting the rest of this chapter in context.

2. Basic Thermospheric Parameters

The thermosphere is the uppermost region of a planet's neutral atmosphere. It is characterised as a region in which the temperature steadily increases with altitude until a maximum (exospheric) limit is reached. Mean free path lengths for thermospheric species are long - sometimes up to hundreds of kilometres - and the mixing of the atmosphere by convection is almost non-existent. The level at which

TABLE I
Key thermospheric parameters for Earth, Jupiter and Saturn

	Earth	**Jupiter**	**Saturn**
Homopause temperature	200 K	200 K	140 K
Homopause pressure	10^{-6} bar	2×10^{-6} bar	1×10^{-7} bar
Homopause density	$3.7 \times 10^{19}\mathrm{m}^{-3}$	$7.3 \times 10^{19}\mathrm{m}^{-3}$	$5.2 \times 10^{18}\mathrm{m}^{-3}$
Homopause scale height[a]	6.0 km	35.7 km	64.5 km
Exospheric temperature	1000 K	940 K	420 K
Exospheric scale height[b]	52.6 km	335.6 km	387.0 km
Critical density	$10^{14}\mathrm{m}^{-3}$	$2.5 \times 10^{13}\mathrm{m}^{-3}$	$2.5 \times 10^{13}\mathrm{m}^{-3}$
Critical pressure	4×10^{-12} bar	10^{-12} bar	10^{-12} bar

[a] Scale height for N_2 for Earth and H_2 for Jupiter and Saturn.
[b] Scale height for O for Earth and H for Jupiter and Saturn.

convective mixing is no longer important is known as the homopause. Above the homopause, atmospheric atomic and molecular species settle out diffusively; each species has its own scale height, H_S, given by:

$$H_S = kT/gm_S \tag{1}$$

where k is Boltzman's constant, T is the thermospheric temperature, g the acceleration due to gravity and m_S is the atomic or molecular weight of species S. At higher altitudes, the thermosphere merges into the exosphere. The base of the exosphere – the *exobase* – is characterised by a critical density, $N_\mathrm{C}(S)$, at which the horizontal mean free path of the main thermospheric species, S, is equal to the scale height. $N_\mathrm{C}(S)$, is given by:

$$N_\mathrm{C}(S) = \left(\pi d_S^2 H_S\right)^{-1} \tag{2}$$

where d_S is the diameter of species S. Some approximate values for key parameters for the Earth, Jupiter and Saturn are compared in Table I.

The above considerations enable more detailed vertical profiles of the thermosphere to be developed. These are shown below for Jupiter (Figure 3; Grodent *et al.*, 2001) and for Saturn (Figure 4; Smith *et al.*, 2004). They show that, except at the very bottom of the thermosphere, where hydrocarbon molecules still have some abundance, the atmosphere is composed mainly of molecular and atomic hydrogen, with helium as a minor species. Diffusive separation ensures that the proportion of H/H_2 increases monotonically with altitude.

To a first approximation, conditions at the homopause are regulated by the balance between the upward convection of heat in the mesosphere and downward conduction of heat in the thermosphere, and the radiation to space of heat from emitting species in the homopause region. More detailed consideration of these

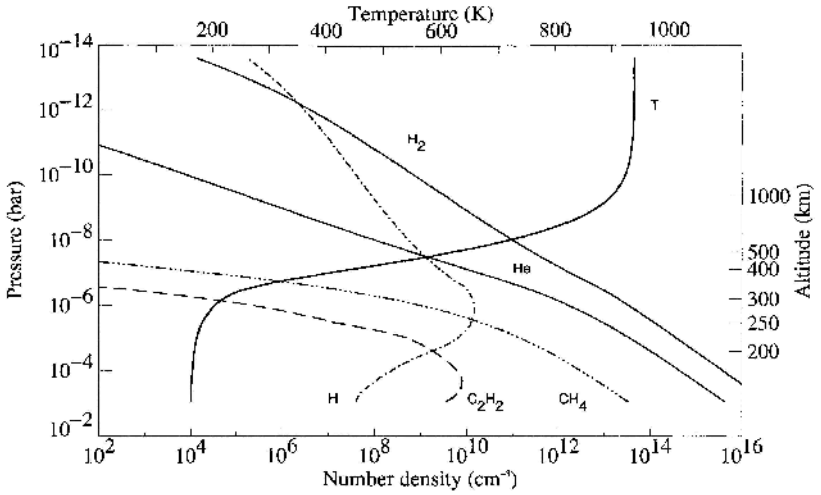

Figure 3. Profile of the composition and temperature profile of the jovian upper atmosphere (from Grodent *et al.*, 2001).

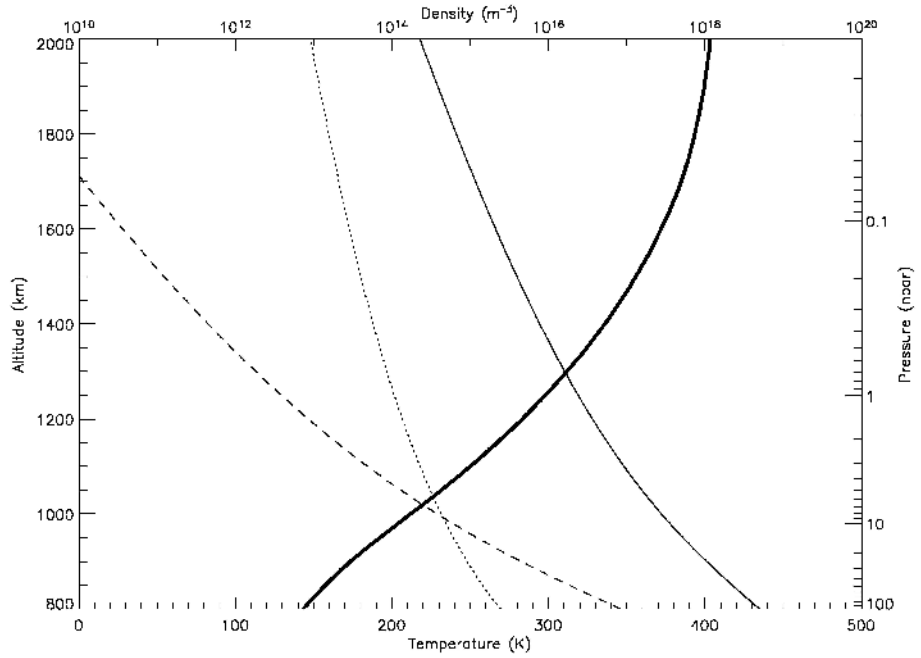

Figure 4. Profile of the composition and temperature profile of the saturnian upper atmosphere (from Smith *et al.*, 2004). *Dark line:* temperature; *light line:* H_2 density; *dashed line:* He density; *dotted line:* H density.

issues can be found in Atreya (1986). In the case of Jupiter, Drossart *et al.* (1993) have shown that hydrocarbons are extremely efficient radiators, emitting some 10^{13} W and controlling the homopause temperature. Above the homopause, the exact temperature profile is determined by a balance between energy inputs as a function of altitude, the downward conduction of heat, and the radiation of heat to space. For Jupiter, this last is due mainly to the efficient radiation of the H_3^+ molecular ion (see Section 3 below; Lam *et al.*, 1997b; Miller *et al.*, 1997; Waite *et al.*, 1997). One key question for all studies of the upper atmospheres of the giant planets is that measured exospheric temperatures are several hundred degrees higher than can be produced by the effects of solar EUV heating alone (Strobel and Smith, 1973; Yelle and Miller, 2004).

3. Basic Ionospheric Considerations

Ionospheres are produced by the impact of ionising radiation and precipitating particles on the neutral atmosphere, and the chemical reactions that ensue. Most of the relevant chemistry for giant planets is summarised in the chapter in this volume by Strobel (2005). More details are given in Waite *et al.* (1983), Majeed and McConnell (1991), and Kim *et al.* (1992). There have also been several reviews, e.g. Atreya (1986), Majeed *et al.* (2004a), Yelle and Miller (2004). Moses and Bass (2000) and Moses *et al.* (2000) have produced an extensive chemical scheme, including all the major reactions involving hydrocarbons, which is particularly appropriate to the lower ionosphere, around and below the homopause. For the purposes of this chapter, however, we shall (mainly) consider only that part of the ionosphere that coexists with the thermosphere. For Jupiter and Saturn that very much simplifies the situation; except at the very bottom of the thermosphere, the chemistry that produces the ionic species is very simple, consisting of reactions between atomic and molecular hydrogen, and helium, and their ionised products. The most important, primary ionisation reactions for the production of the (upper) ionosphere are then:

$$H + h\nu/e^* \rightarrow H^+ + e \ (+e) \quad \text{(I1)}$$

$$H_2 + h\nu/e^* \rightarrow H_2^+ + e \ (+e) \quad \text{(I2a)}$$

$$\rightarrow H^+ + H + e \ (+e) \quad \text{(I2b)}$$

$$H_2^+ + H_2 \rightarrow H_3^+ + H \quad \text{(I3)}$$

$$He + h\nu/e^* \rightarrow He^+ + e \ (+e) \quad \text{(I4)}$$

Reaction I3 follows on so rapidly from reaction I2a that H_2^+ is almost non-existent in the jovian and saturnian ionospheres. The effect is that H_3^+ is the main molecular ion (Figure 5), and – in the auroral regions in particular – can be the major ionospheric species. A further reaction of importance involves charge exchange:

$$H^+ + H_2 \ (v \geq 4) \rightarrow H_2^+ + H \quad \text{(E1)}$$

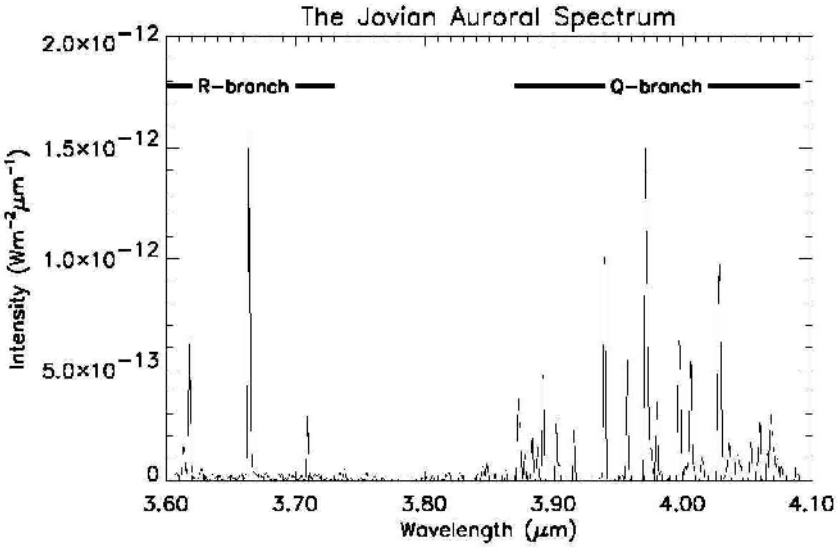

Figure 5. Spectrum of Jupiter's northern aurora in the 3.5 to 4 μm region showing the strong H_3^+ emission (Stallard and Miller, unpublished data).

in which the difference in ionisation energy of H (13.6 eV) and H_2 (15.4 eV) is made up by making use of vibrationally excited molecular hydrogen. Since E1 leads into I3, the net result is to enhance the concentration of H_3^+ at the expense of H^+. Majeed *et al.* (1991) show that this is an important reaction, if levels of vibrationally excited H_2 are overpopulated, compared with what could be expected from LTE, by resonant fluorescence. Unfortunately, the rate of charge exchange for E1 is not well constrained, even to within an order of magnitude (see discussion by Moses and Bass, 2000). Recent work by Moore *et al.* (2004) has shown that this reaction rate can make a large difference to the H^+/H_3^+ balance in the ionosphere. The final component in determining ionospheric concentrations is recombination. For H^+ and He^+, only radiative attachment, the reverse of I1 and I4, is significant:

$$H^+/He^+ + e \rightarrow H/He + h\nu \qquad \text{(R1)}$$

But for H_3^+, as for other (hydrocarbon) molecular ions, dissociative recombination is the main mechanism for re-neutralising the ionosphere:

$$\begin{aligned} H_3^+ + e &\rightarrow H_2 + H \\ &\rightarrow H + H + H \end{aligned} \qquad \text{(R2)}$$

This latter reaction is much faster than R1. The main effect of this is that, while on the dayside the predominant equatorial ion may be H^+ or H_3^+, the predominant nightside ion is H^+, with H_3^+ column densities several times lower. Table II shows typical modelled ion column densities for Jupiter and Saturn, calculated for simple $H/H_2/He$ atmospheres.

TABLE II
Modelled Column Densities of H^+ and H_3^+.

	Equatorial Noon	**Equatorial Midnight**
Jupiter[a]		
H^+	$5 \times 10^{15} m^{-2}$	$5 \times 10^{15} m^{-2}$
H_3^+	$9 \times 10^{15} m^{-2}$	$2 \times 10^{15} m^{-2}$
Saturn[b]		
H^+	$6 \times 10^{15} m^{-2}$	$6 \times 10^{15} m^{-2}$
H_3^+	$2 \times 10^{15} m^{-2}$	$0.2 \times 10^{15} m^{-2}$

[a] From Achilleos *et al.* (1998).
[b] From Smith *et al.* (2004).

In the auroral regions, where particle precipitation is important, ion column densities are often an order of magnitude greater than those produced by solar EUV ionisation. The altitude at which the maximum numbers of ions are produced depends critically on the individual energy of the incoming particles; the number of ions depends on the number of incoming particles. These effects are shown for Jupiter in Figures 6 and 7 (Millward *et al.*, 2002), for electron energies in the range of $10 - 100$ keV and fluxes of 0.1 to 1000 mW m^{-2}. Reviews of the comparison of model electron and ion density profiles and spacecraft measurements may be found in Atreya (1986) and in Majeed *et al.* (2004a).

The combination of solar EUV ionisation and particle precipitation gives rise to spatial variations in ion column densities. Figure 8 shows that the column density of jovian H_3^+, measured at local noon, varies by more than an order of magnitude between the auroral regions and the equator (Lam *et al.*, 1997b; Miller *et al.*, 1997). The temperature structure is closely correlated with ionospheric variations, since many of the processes associated with ion chemistry are exothermic. However, there can also be heat transport from one region to another that complicates the picture. A jovian temperature map corresponding to Figure 8 is shown in Figure 9. The highest temperatures are to be found in the auroral/polar regions, > 900 K. But then there is a mid-to-low latitude region that is 150 K or more cooler, before the temperature rises again around the equator. The cooling effect of H_3^+ can be obtained from calculating the overall emission, and ranges from a few milliwatts per square metre in the auroral regions to an order of magnitude less at the equator.

4. Auroral and Polar Cap Mechanisms

Bright aurorae are produced when charged particles are accelerated along magnetic field lines and precipitate from the magnetosphere into the upper atmosphere; the

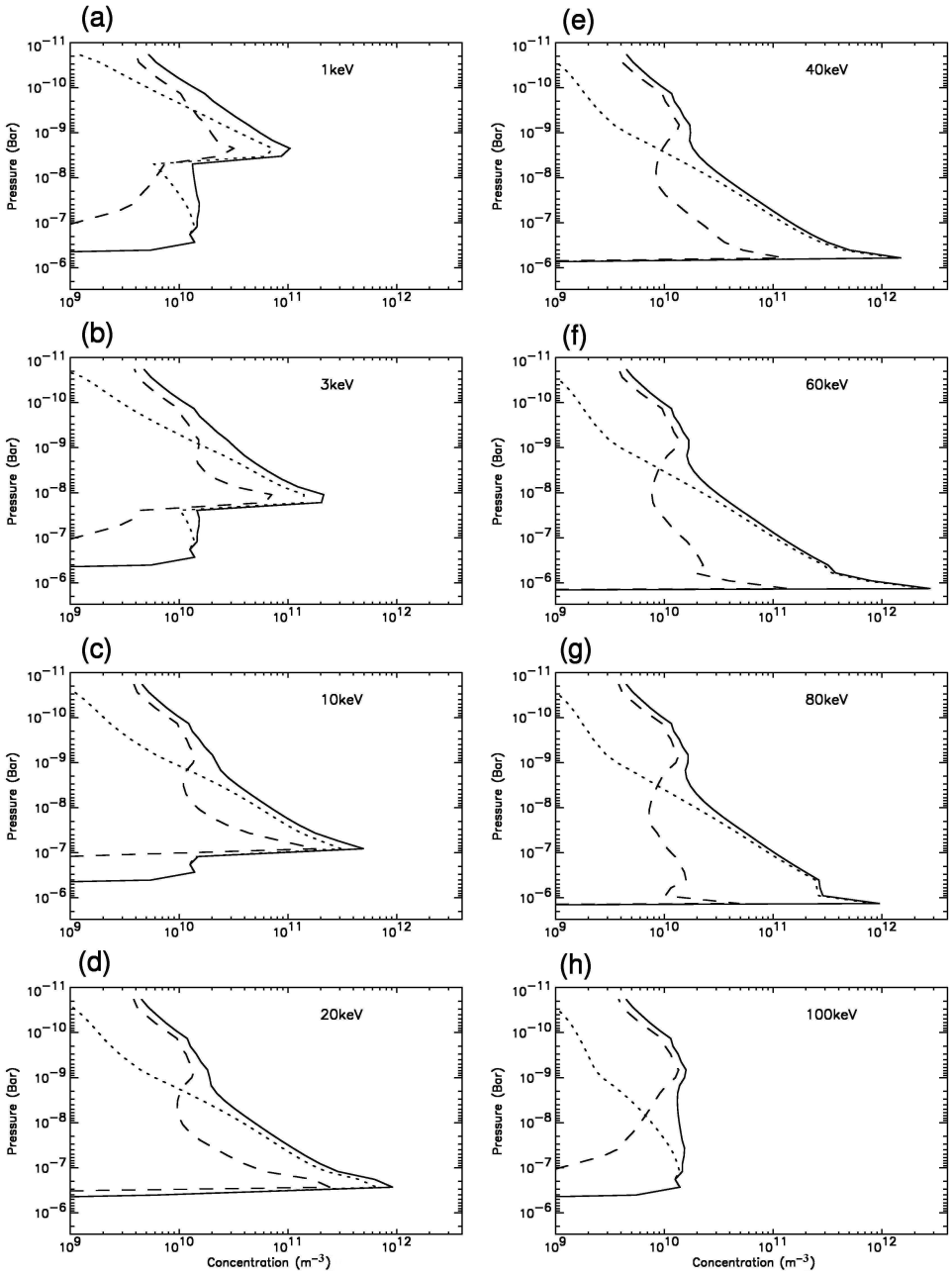

Figure 6. Jovian ion and electron density profiles modelled for a flux of $6.25 \times 10^{12}\mathrm{cm}^{-2}\mathrm{s}^{-1}$ precipitating electrons of various energies. *Full line:* electron density; *dashed line:* H^+ density; *dotted line:* H_3^+ density (from Millward *et al.*, 2002).

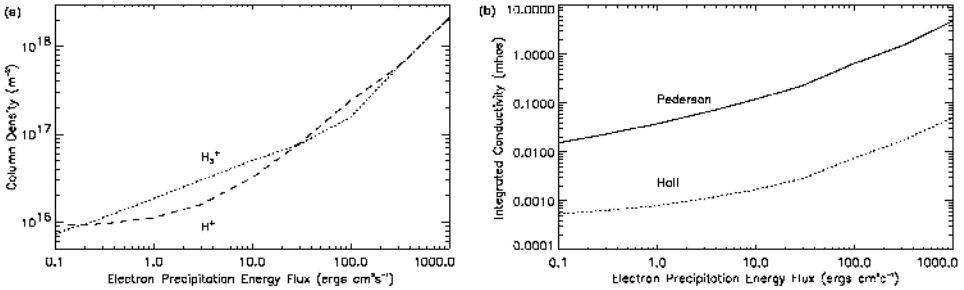

Figure 7. Jovian ion column densities (*top panel*) and conductivities (*lower panel*) modelled for varying total energy fluxes of 10keV electrons (from Millward *et al.*, 2002).

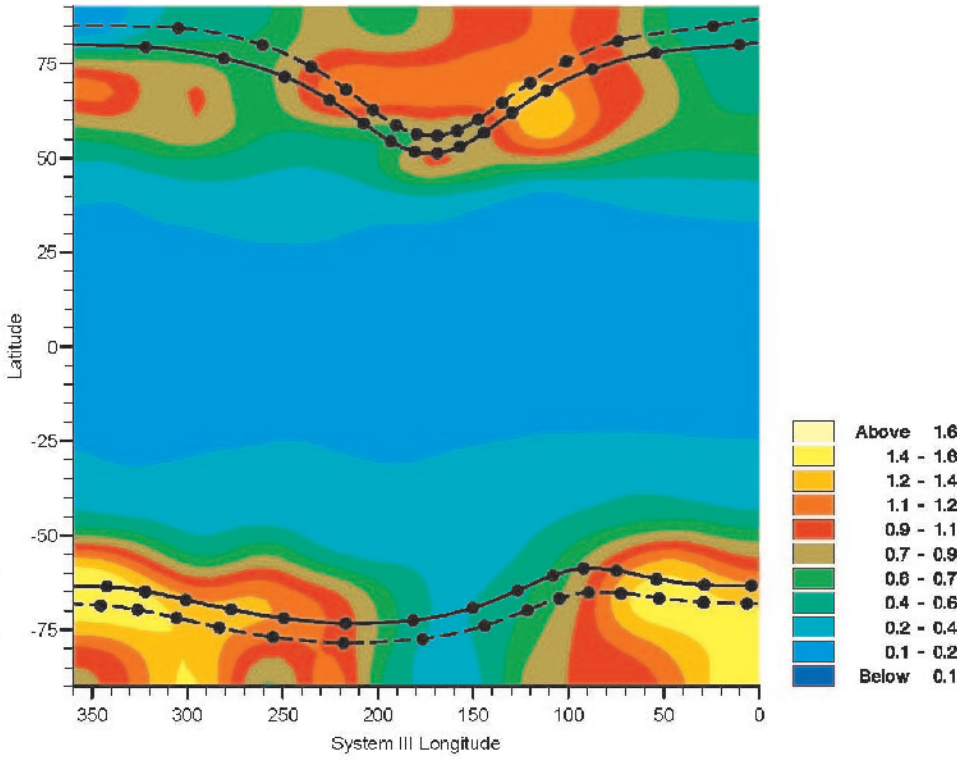

Figure 8. Measured H_3^+ column densities at local noon as a function of location on Jupiter. The units are 10^{12} cm^{-2} (from Lam *et al.*, 1997b).

locations of these aurorae map to the footprints of the fields lines along which the particles have been accelerated. Issues concerning acceleration are dealt with in the chapter by Kivelson (2005), but it is worth considering a few basic points here.

The precipitated particles required to power the Earth's aurorae are equivalent to around 10^{11} W – 10^{12} W (100 GW – 1 TW), and the energy radiated is $\sim 1 - 300$ GW (see Waite and Lummerzheim, 2002). The main auroral oval on

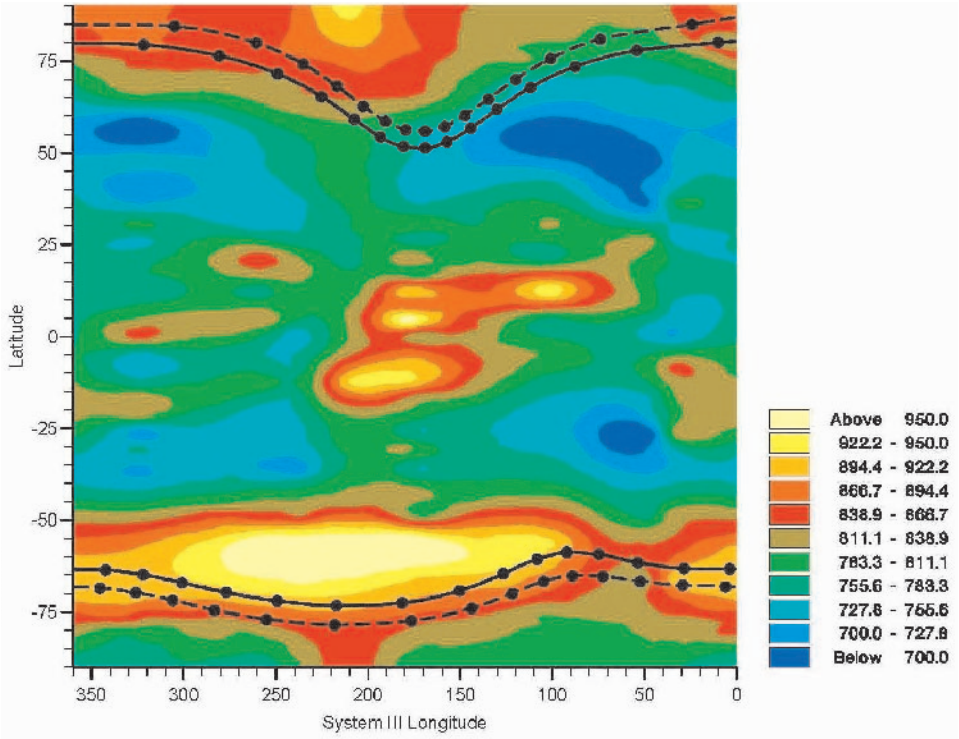

Figure 9. Measured H_3^+ temperatures at local noon as a function of location on Jupiter (from Lam *et al.*, 1997b).

the Earth occurs close to the footprint of the boundary between open and closed magnetic field lines where, in the magnetosphere, currents are generated due to the discontinuity in the flow of plasma. The location of this boundary depends on the solar wind and the interplanetary magnetic field. The main driver of the Earth's aurorae is the interaction with the external medium of the solar wind. In the upper atmosphere, poleward of the main oval – i.e. in the polar cap – field lines are dragged anti-sunward by the solar wind across the poles, returning in the sunward direction along the flanks of the oval. This Dungey cycle (Dungey, 1961) lasts about 3 hours, around an eighth of the Earth's rotation period. The Earth's aurora and polar cap are thus said to be solar wind controlled.

This is not the situation for Jupiter. The innermost Galilean moon, Io, which orbits at 5.9 jovian radii (R_J, $1R_J = 71,343$ km) emits about 1 tonne per second from its volcanoes. The neutral gases emitted are initially rotating with the Keplerian orbital period, ≈ 42.5 hours, and are subsequently ionised. The ions so produced are then swept up by Jupiter's magnetic field into an equatorial plasma sheet, which co-rotates with the planet once every 9 hours 55 minutes, and driven centrifugally outwards, a process which requires angular momentum to be transferred from the ionosphere, via a current system. At a radial distance between $\sim 20 - 30R_J$,

corotation begins to break down (Hill, 1979). Field-aligned voltages are generated above the ionosphere that accelerate (mainly) electrons to keV energies along the field lines connecting to the region of corotation breakdown in the plasma sheet, generating the main auroral oval (Cowley and Bunce, 2001; Hill, 2001). Thus the driver for the main auroral oval on Jupiter is internal – the equatorial plasma sheet. Jupiter's aurorae are therefore said to be controlled rotationally, rather than by the solar wind. The energy input of precipitated particles ($\sim 10 - 100$ TW) and the radiated auroral energy ($3 - 10$ TW) are both ~ 100 times greater than the situation for the Earth (Atreya, 1986; Clarke *et al.*, 1987; Waite and Lummerzheim, 2002). Equatorward of the main oval, aurorae due the Galilean moons have been discovered (Connerney *et al.*, 1993, Clarke *et al.*, 1998; 2002; Prangé *et al.*, 1998). Around the magnetic poles, regions equivalent to the Earth's polar cap, i.e. under the control of the solar wind, have been identified (Pallier and Prangé, 2001; Stallard *et al.*, 2003) and analysed (Cowley *et al.*, 2003). Between the main oval and the polar cap, other auroral emissions are seen (see Figures 1a and 2a, and chapter by Kivelson, 2005).

The Voyager 2 spacecraft found auroral emission on Uranus, located around the magnetic poles (Broadfoot *et al.*, 1986; see Herbert and Sandel, 1994, for a full analysis). Unlike Jupiter, however, Uranus does not appear to exhibit localised auroral emission in the H_3^+ infrared (Figure 2b). Instead it has a rather uniform distribution across the disk, peaking at the sub-solar point, with any auroral enhancement probably not more than 20% of the average disk emission (Trafton *et al.*, 1999). As Figure 1b shows, Saturn has a well defined, if variable and non-uniform, auroral oval visible in UV radiation. Until recently, the origin of this oval was unknown. However, recent theoretical work has proposed that it corresponds – as in the case of the Earth – to the closed-open field line boundary (Cowley *et al.*, 2004). Typically, some ~ 100 GW of precipitating electrons are required to produce the ~ 10 GW aurorae, although these may be as feeble as 100×10^6 W (100 MW) on occasions (Trauger *et al.*, 1998). Poleward of the main auroral oval may be flows corresponding to the Dungey cycle, and that predicted by Vasyliunas (1983) (Figure 10). Cowley *et al.* (2004) predict that the Dungey cycle on Saturn takes ≈ 50 hrs, about five times longer than the planetary rotation period.

5. Measurement and Modelling of Ion and Neutral Dynamics

In the past few years there have been significant developments in the measurement and modelling of dynamics in the upper atmospheres of giant planets. In particular, high resolution infrared spectra of Jupiter have revealed the presence of ion winds. These can be driven by magnetospherically generated fields (Rego *et al.*, 1999; Stallard *et al.*, 2001) and by the solar wind (Cowley *et al.*, 2003; Stallard *et al.*, 2003). Three-dimensional modelling, using the Jovian Ionospheric Model (JIM; Achilleos *et al.*, 1998), has demonstrated that such ionospheric flows can couple

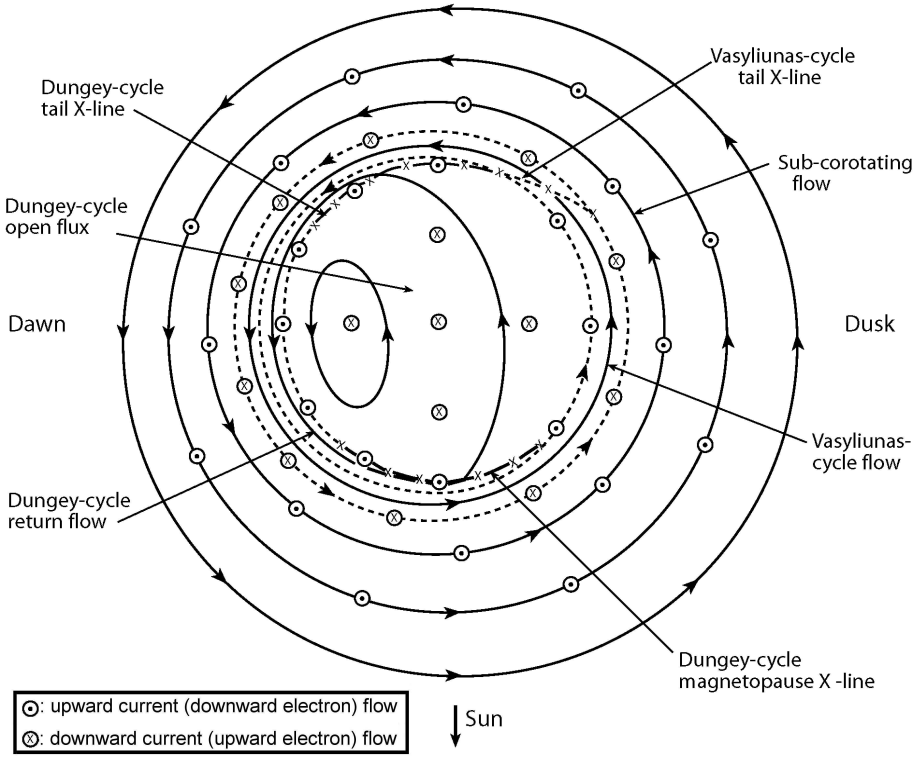

Figure 10. Predicted polar ion flows on Saturn (from Cowley *et al.*, 2004).

to the neutral atmosphere to produce strong wind systems (Millward *et al.*, 2004), which may be responsible for transporting energy from the auroral/polar regions as originally suggested some twenty years ago by Waite *et al.* (1983). Similar results have been obtained using the Jupiter Thermosphere Global Circulation Model of Majeed *et al.* (2004b).

The measurement of ion winds has been achieved by looking at the Doppler shifting of infrared emission from the H_3^+ molecular ion, using NASA's Infrared Telescope Facility and the high-resolution, long-slit spectrometer. Much work has been carried out on Jupiter (Rego *et al.*, 1999; Stallard *et al.*, 2001; 2003) during the time of the Galileo Mission. Figure 11 shows an intensity profile of the $H_3^+ \nu_2 Q(1, 0^-)$ line at 3.953 μm, measured west-east across the auroral oval and polar cap. The profile shows structure corresponding to the auroral oval (Rising and Setting Auroral Oval; RAO and SAO) and regions poleward of that (Dark and Bright Polar Regions; DPR and BPR). It is still unexplained as to why even the DPR still has some 40% of the brightness of the auroral oval when viewed in H_3^+ emission, although this region is very dark when viewed in the UV (Pallier and Prangé, 2001). Figure 12 shows the corresponding line-of-sight (l.o.s.) velocity profiles in the frame of reference that corotates with the planet. It is immedi-

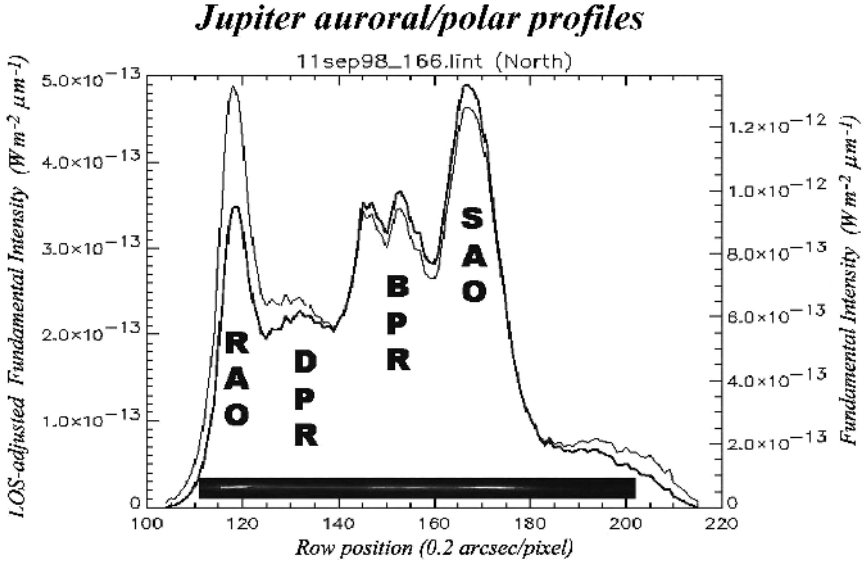

Figure 11. Measured H_3^+ emission profile across the jovian auroral oval (from Stallard *et al.*, 2001). The light line shows the intensity of the 3.953 μm emission as measured; the dark line shows the emission corrected for line-of-sight. RAO: Rising Auroral Oval; DPR: Dark Polar Region; BPR: Bright Polar Region; SAO: Setting Auroral Oval.

ately noticeable that the SAO is blue-shifted and the RAO red-shifted, each by ≈ 1 km s^{-1}. This corresponds to an auroral electrojet with a velocity ≈ 1.5 km s^{-1} flowing (clockwise as viewed from above the north pole) around the auroral oval, counter to the rotation of the planet.

The explanation of this electrojet flows naturally from the Hill (1979) mechanism by which the main auroral oval emission is generated. The electric field, $\mathbf{E}_{\rm eqw}$, that drives the equatorward current through the ionosphere, to close the plasma sheet/field-line/atmosphere circuit, couples with the (near-vertical) jovian auroral magnetic field, $\mathbf{B}_{\rm aur}$, to produce a retrograde Hall ion drift at right angles to both $\mathbf{E}_{\rm eqw}$ and $\mathbf{B}_{\rm aur}$:

$$\mathbf{v}_{\rm ion} = \mathbf{E}_{\rm eqw} \times \mathbf{B}_{\rm aur}/|\mathbf{B}_{\rm aur}|^2 \ . \tag{3}$$

Since the magnetic field in the auroral regions is $\sim 10^{-3}$ Tesla, a velocity of 1.5 km s^{-1} corresponds to $E_{\rm eqw} \approx 1.5$ V m^{-1}. Higher velocities, up to twice this amount, have also been noted (Rego *et al.*, 1999). Integrated across the width of the auroral oval, which can easily be between 500 km and 1000 km as measured by the H_3^+ intensity profiles, it is clear to see that $V_{\rm eqw}$ – the potential difference generated across the oval by the fields in the plasma sheet – can be of the order of a megavolt or more. Such potential differences are in line with those predicted by theory (Cowley and Bunce, 2001).

Millward *et al.* (2004) have used JIM (Jovian Ionospheric Model; Achilleos *et al.*, 1998) – which is a fully coupled ionosphere-thermosphere global circulation

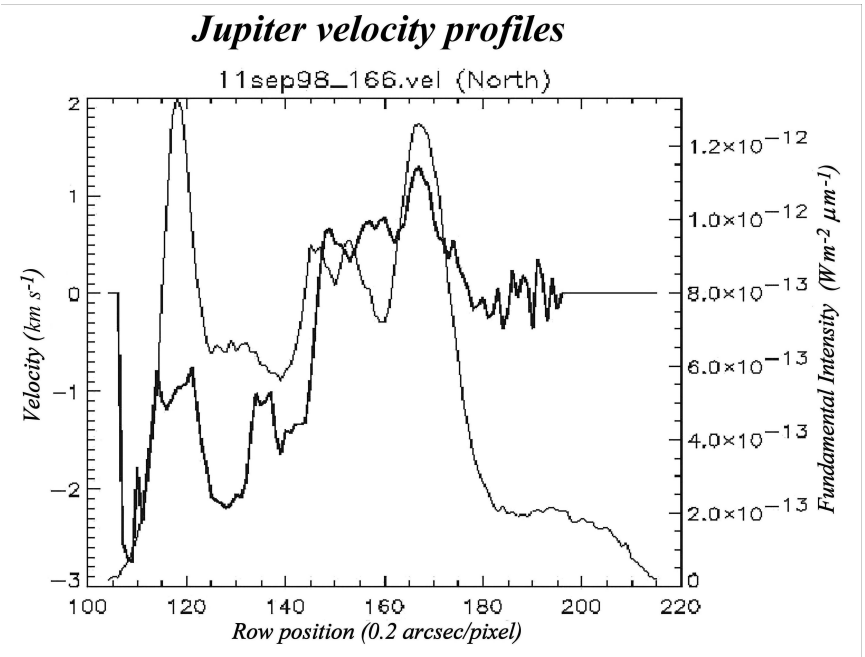

Figure 12. Measured H_3^+ l.o.s. velocity profile across the jovian auroral oval (from Stallard *et al.*, 2001) (*dark line*). The intensity profile (*light line*) is overplotted to aid visualisation. The RAO is red-shifted and the SAO blue-shifted in the planetary reference frame denoting the retrograde auroral electrojet. The strong re-shifting of most of the DPR is consistent with ions that are held near-stationary in the frame of reference that rotates with the magnetic pole (Stallard *et al.*, 2003).

model – to calculate the dynamics of the upper atmosphere under the influence of such equatorward voltages. Coupling to the local magnetic field, electric fields of 2.0 V m^{-1} produce an ion drift of $\approx$1.6 km s^{-1} in the rest frame of the planet. At the peak of the ion concentration – around 1 μbar for 60 keV electron precipitation (see Figure 6) – the neutrals are entrained by collisions with ions so efficiently that a neutral wind of $\approx$1 km s^{-1} is produced. For smaller voltages, e.g. 0.6 V m^{-1}, the Hall drift is around 500 m s^{-1} and the neutral wind $\approx$350 m s^{-1}. A parameter $K(h)$ may be defined such that:

$$K(h) = |v_{\text{neut}}(h)/v_{\text{ion}}(h)| \tag{4}$$

for any altitude, h (Huang and Hill, 1989). $K(h)$ thus represents the fraction of the ion velocity, in the planetary reference frame, that is acquired by the neutrals via ion-neutral collisions. For the upper atmosphere, where eddy diffusion is almost negligible, JIM results show that $K(h)$ peaks strongly at the level that the ion density peaks, with a value of 0.5 or greater. This parameter is used by Cowley and Bunce (2001) in a height-independent form to modify the height-integrated

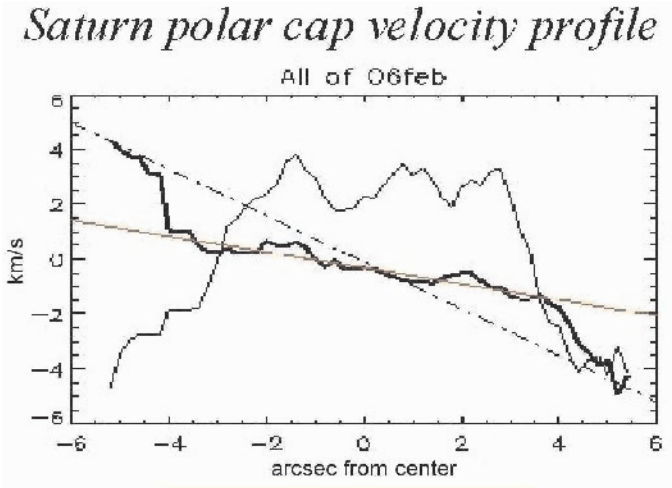

Figure 13. Measured H_3^+ l.o.s. velocity profile across the saturnian auroral oval (from Stallard *et al.*, 2001) (*dark line*) in the inertial reference frame. The intensity profile (*light line*) is overplotted to aid visualisation. The dash-dot line shows the line of corotation with the planet; the red line shows the best straight line fit to the measured velocity profile, only 0.34 of the planetary angular velocity.

Pedersen conductivity of the ionosphere, to allow for the relative motions of ions in the rest frame of the neutral atmosphere in which they are located by:

$$\Sigma_P^* = (1 - K)\Sigma_P \quad . \tag{5}$$

With a view to the Cassini Mission, Stallard *et al.* (2004) have recently extended their technique for measuring ion winds on Jupiter to Saturn. Unfortunately, Saturn's auroral emissions – in both UV and IR (H_3^+) – are only a few percent of those of Jupiter. For high resolution IR spectroscopy, this means that exposure times for Saturn are ≈ 1 hour, or more, compared with ≈ 1 minute for Jupiter. Such long exposure times would not be feasible for Jupiter, because of the large offset of the magnetic and rotational poles: auroral intensity and velocity features would be "smeared out" by the rotation of the planet ($\approx 0.6^\circ$ of longitude per minute, or 36° in an hour) to such an extent as to defy analysis. Fortunately, the magnetic and rotational poles of Saturn are near-coincident, and average parameters may still be obtained from hour-long exposures, without longitudinal smearing being too problematic.

Figure 13 shows the velocity profile of Saturn obtained in 2003. This led Stallard *et al.* (2004) – independently – to the same conclusion that Cowley *et al.* (2004) had reached from theoretical considerations: the polar cap region of Saturn is largely under solar wind control, causing the ions there to rotate much more slowly than the planet (in the Sun-Saturn reference frame). The measured average angular velocity of the polar cap ionosphere was $0.34\Omega_S$, where Ω_S is the angular velocity of Saturn, compared with a theoretical prediction of $0.24\Omega_S$. The interpretation of these ion winds is that an equatorward field is imposed by the tendency of

TABLE III
Comparison of predicted and measured exospheric temperatures.

	Jupiter	**Saturn**	**Uranus**	**Neptune**
Heliocentric distance (AU)	5.20	9.57	19.19	30.07
Absorbed solar flux (W m^{-2})	3.7×10^{-5}	1.1×10^{-5}	2.7×10^{-6}	1.1×10^{-6}
$T_{\rm exo}$ (observed) [K]	940	420	800	600
$T_{\rm exo}$ (calculated) [K]	203	177	138	132
$\Delta T_{\rm exo}$ (obs-calc) [K]	737	243	662	468

the solar wind to sweep open field lines down the magnetotail, and prevent them rotating with the planet. At the edge of the polar cap, which extends to a colatitude of $\approx 15^\circ$, the ion wind is ≈ 1.7 km s^{-1}. With Saturn's auroral magnetic field being $\approx 6.5 \times 10^{-5}$ Tesla (Cowley *et al.*, 2004), Equation (3) gives the field strength ≈ 0.1 V m^{-1}. Cowley *et al.* (2004) also relate the measured ion angular velocity to the solar wind velocity and the effective Pedersen conductivity:

$$\Omega_{\rm ion} = \Omega_S \mu_0 \Sigma_{\rm P}^* V_{\rm SW} / \left[1 + \mu_0 \Sigma_{\rm P}^* V_{\rm SW}\right] \tag{6}$$

where μ_0 is the permeability of free space, and $V_{\rm SW}$ is the solar wind velocity. This important relationship, first derived by Isbell *et al.* (1984), holds out the prospect of correlating the measured ion velocities with Cassini measurements of the solar wind velocity, and thereby measuring conductivities, which can be modelled to derive particle precipitation fluxes. Alternatively, in the absence of available spacecraft data, the measured values of $\Omega_{\rm ion}$ may be used, with modelled conductivities, to obtain values of $V_{\rm SW}$.

6. Energy Considerations

Yelle and Miller (2004) have recently compared the measured exospheric temperatures of the giant planets with those calculated from solar EUV inputs alone. Globally, the solar EUV absorbed at Jupiter is ≈ 2.4 TW, while at Saturn it is ≈ 0.5 TW. Table III shows that considerable additional energy sources are required to produce the observed temperatures.

Particle precipitation in Jupiter's auroral/polar regions is estimated to provide an additional 10 to 100 TW (Clarke *et al.*, 1987), a considerable increase on the solar EUV input, although a large fraction of that may be deposited below the homopause, from where much of the UV auroral radiation emanates; below the homopause – as already noted – hydrocarbons radiate away the energy very efficiently (Drossart *et al.*, 1993). That means that the actual direct energy input into the upper atmosphere (above the homopause) is probably less than 10 TW globally. Grodent

et al. (2001) have produced a 1-dimensional self-consistent model of the jovian upper atmosphere from 20 mbar – i.e. below the homopause – to 10^{-13} bar, well into the lower exosphere (see Figure 3). Their model requires $\approx 3 \times 10^{-2}$ W m^{-2} to produce an auroral temperature profile consistent with UV and IR observations and the low latitude temperature profile measured by the Galileo probe (Seiff *et al.*, 1998). The energy, in the form of keV electrons for the most part, has to be deposited at various altitudes in order to produce the correct temperature profiles. If one approximates the jovian auroral oval to a circle at co-latitude 15° and 500 km wide, the Grodent *et al.* inputs correspond to $3 - 4$ TW globally. There is probably a similar amount from what they term "diffuse aurora", found (mainly) poleward of the main auroral oval.

To produce the high temperatures measured globally, Waite *et al.* (1983) proposed that thermally driven winds could distribute the large amounts of energy deposited in the auroral regions. But such winds have powerful Coriolis forces to overcome as a result of Jupiter's rapid rotation. A solution to the "energy gap" that may be available globally is breaking waves, generated in the lower atmosphere and depositing their energy in the thermosphere (Young *et al.*, 1997). Matcheva and Strobel (1999), however, have questioned whether waves can deposit enough energy to account for the high jovian thermospheric temperatures measured by the Galileo probe (Seiff *et al.*, 1998), and there are even claims that gravity waves may actually cool the upper atmosphere (Hickey *et al.*, 2000). The situation for Saturn, with respect to wave propagation from the lower atmosphere, is currently unclear. But, without identifying what the source of heating is, Mueller-Wodarg *et al.* (2004) have shown that a global energy input to the lower thermosphere of Saturn can increase the exospheric temperature from the ≈ 180 K predicted from solar heating alone to ≈ 410 K, in close agreement with the measurements of Smith *et al.* (1983).

There is some evidence from UV (Feldman *et al.*, 1993), IR (Miller *et al.*, 1997; Rego *et al.*, 2000) and X-ray (Waite *et al.*, 1997) emissions from Jupiter that particle precipitation occurs equatorward of the jovian auroral regions to latitudes as low as 20°, or even to the equator. Such low latitude particle precipitation has been modelled recently by Abel and Thorne (2003) for relativistic particles; they find that IR emission patterns in the northern hemisphere are fairly well reproduced by their model. Such precipitation would heat the atmosphere outside of the auroral regions, and it is worth noting that Grodent *et al.* (2001) require a low energy electron "drizzle" to keep their upper thermospheric temperatures in agreement with the Galileo probe profile. On the other hand, Liu and Dalgarno (1996) modelled the equatorial UV dayglow from Jupiter (Feldman *et al.*, 1993) and found that solar EUV radiation alone could generate the observed spectrum, without the need for additional excitation, such as would be produced by particle precipitation. Planetwide precipitation is probably required to produce the distribution of H_3^+ emission (Figure 2b) observed on Uranus (Trafton *et al.*, 1999). Theoretical

considerations also indicate that low-intensity particle precipitation may occur on Saturn at latitudes lower than the main auroral oval (Cowley *et al.*, 2004).

However, there are two other sources of energy that may be produced within the upper atmosphere, above the homopause, close to the ionisation peak, which would not generate additional UV radiation: Joule heating and "frictional" heating. These are not readily incorporated into 1-D models such as that of Grodent *et al.* (2001).

Joule heating is generated by the passage of currents in the ionosphere. An early attempt to quantify its significance was carried out by Heaps (1975), who concluded that it was less important for Jupiter than for the Earth. However, these calculations were based on relatively low values of electric fields and ionospheric conductivity, more suitable to non-auroral latitudes. The amount of heating produced in the jovian auroral oval by the equatorward electric field discussed above is given by:

$$H_{\rm J} = |(1-K)E_{\rm eqw}|^2\, \Sigma_{\rm P}\, A_{\rm oval} \tag{7}$$

where $A_{\rm oval}$ is the area of the oval, and the factor $(1-K)$ is required to calculate the Joule heating produced by the current flowing in the rest frame of the neutral atmosphere. Millward *et al.* (2002; 2004) have shown that plausible electron fluxes produce values of $\Sigma_{\rm P}$ of 1-8 mho. Approximating the oval as before – which gives $A_{\rm oval} = 5.7 \times 10^{13}$ m^2 – and taking $E_{\rm eqw}$ to be 1.5 V m^{-1} in the planetary rest frame and $K = 0.5$ (Millward *et al.*, 2004), Joule heating can be seen to produce 130 TW per hemisphere for $\Sigma_{\rm P} = 4$ mho. This is about 200 times more than that first considered by Heaps (1975). (Note that in calculating this figure we have not taken into account any Joule heating produced poleward of the auroral oval by the fields that must exist there to produce the observed ion flows.)

It is possible to carry out a similar calculation for the auroral/polar regions of Saturn, making use of the measured magnetic field and ion lag to corotation, and estimating the effective conductivity. Approximating the auroral oval to a circle centred on the rotational pole with a co-latitude of 15°, we have:

$$\begin{aligned} H_{\rm J} &= \int_0^{R_{\rm oval}} |(1-K)E_{\rm eqw}(r)|^2 \Sigma_{\rm P} 2\pi r\,{\rm d}r = \int_0^{R_{\rm oval}} |(1-K)Bv_{\rm ion}(r)|^2 \Sigma_{\rm P} 2\pi r\,{\rm d}r \\ &= \int_0^{R_{\rm oval}} |(1-K)B\Omega_{\rm ion} r|^2\, \Sigma_{\rm P}\, 2\pi r\,{\rm d}r = \frac{\pi}{2} |(1-K)B\Omega_{\rm ion}|^2\, \Sigma_{\rm P}\, R_{\rm oval}^4 \end{aligned} \tag{8}$$

where we have assumed that B, $\Omega_{\rm ion}$ and $\Sigma_{\rm P}$ are constant across the polar cap, and $R_{\rm oval}$ is $R_S \sin(15°)$ ($R_S = 60,268$ km). For the measured ion angular velocity, and assuming $B = 6.5 \times 10^{-5}$ T and $\Sigma_{\rm P} = 1$ mho, we have $H_{\rm J} \approx 4$ TW in each hemisphere, if $K = 0.1$. This is similar to the value calculated by Cowley *et al.* (2004), using a more sophisticated model of the magnetic field and plasma flows. (Note values of K have not been modelled for Saturn yet, and this low value is taken since the degree of ionisation in the saturnian ionosphere is lower than for Jupiter.)

Modelling the effects of ion-neutral collisions has shown that, while the ions respond immediately to the imposition of an equatorward electric field, neutrals take $\sim$ 1000 s to reach their terminal velocity, and a similar time to decelerate when the field is removed (Miller *et al.*, 2000; Millward *et al.*, 2004). This prompted Miller *et al.* (2000) to ask whether the mechanical (kinetic) energy stored up in large-scale neutral wind flows could also provide a source of energy for heating the upper atmosphere, via some sort of "frictional" effect. For Jupiter, the total kinetic energy in the auroral oval is given by:

$$\text{K.E.} = \frac{1}{2} m_{\text{oval}} v_{\text{neut}}^2 = \frac{1}{2} A_{\text{oval}} \rho_{\text{air}} (K v_{\text{ion}})^2 \tag{9}$$

where ρ_{air} is the column mass of jovian air above the ion peak, which is 4×10^{-2} kg m^{-2}, for ion peak produced by 60keV electron precipitation. Using the parameters given above, and $K = 0.5$, we get K.E. $= 5.7 \times 10^{17}$ Joules per hemisphere. The half-life of 1000 s for neutrals to accelerate and decelerate suggests that this could provide $\approx$ 300 TW per hemisphere, if all of the energy dissipated ended up as heat. For Saturn's polar cap the kinetic energy is given by:

$$\text{K.E.} = \frac{1}{2} \int_0^{R_{\text{oval}}} 2\pi r \rho_{\text{air}} (r \Omega_{\text{ion}} K)^2 \, \mathrm{d}r = \frac{1}{4} \pi \rho_{\text{air}} \Omega_{\text{ion}}^2 R_{\text{oval}}^4 K^2 \ . \tag{10}$$

Taking ρ_{air} as 10^{-3} kg m^{-2} for Saturn and the parameters used previously, we have K.E. $= 5.5 \times 10^{17} \times K^2$ J per hemisphere. Taking again $K = 0.1$, one would have K.E. $= 5.5 \times 10^{15}$ J per hemisphere. This could produce – using arguments similar to those used for Jupiter above – a contribution of 3 TW per hemisphere of additional energy.

Recent calculations using JIM have demonstrated that ion-neutral coupling in Jupiter's auroral oval can generate waves that transport energy to low latitudes. These are shown in Figure 14, for a model run in which the equatorward potential difference across the auroral oval was set to 3 MV, equivalent to $\approx$ 0.6 V m^{-1}. Smith *et al.* (2004) have modelled the effect of putting energy into the polar cap of Saturn at various altitudes. They take into account the measured temperatures of $350 - 500$ K at the ion peak in the auroral/polar region (Melin *et al.*, 2004) and the equatorial exospheric temperature of 420 K (Smith *et al.*, 1983). They find that a few TW input at the ion peak can produce heating of the entire thermosphere to give the measured equatorial exospheric temperature, as a result of conduction and adiabatic heating. The latitudinal temperature profile is similar to that measured for Jupiter (Lam *et al.*, 1997b; Miller *et al.*, 1997). Thus auroral/polar heating, produced by Joule heating or "frictionally", may well heat the entire upper atmosphere for Jupiter and Saturn.

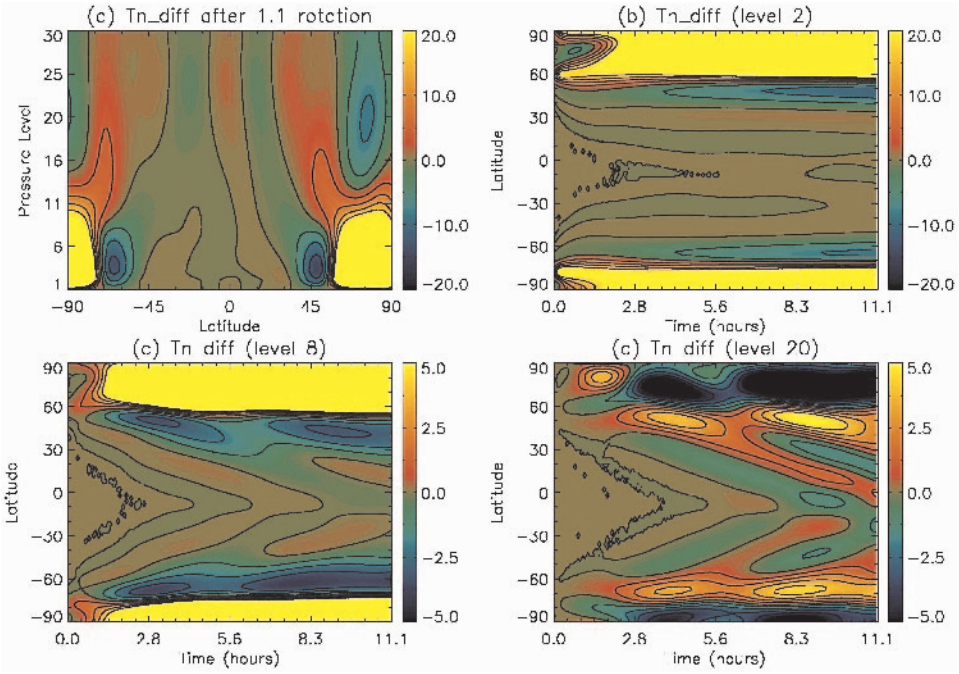

Figure 14. JIM prediction of planet-wide temperature waves generated by the coupling between accelerated ions in the auroral oval and the co-existing thermosphere, as a function of pressure level (*top left*) and time. The plots show the difference between a run carried out with a 3 MV potential difference across the auroral oval (≈ 0.6 V m^{-1}) and one with no p.d. For JIM, Pressure Level 1, $P(1)$, corresponds to 2 mbar, and the models runs on a logarithmic pressure scale such that $P(n) = P(1)\exp[-0.4(n-1)]$. This gives $P(2) = 1.34$ mbar, $P(8) = 0.12$ mbar, and $P(20) = 1.00$ nbar.

7. Conclusions

This brief overview of the upper atmospheres of Jupiter and Saturn shows that, while much has been learned in recent years, there are many outstanding issues for both planets (as for all of the outer planets). One area of great interest is the role of the solar wind in determining the strength and morphology of auroral features in the giant planets – in Jupiter's case, inside the main oval in the polar cap, and for Saturn, the main oval itself. This area of research has been given more impetus with the discovery of a solar wind modulation of Jupiter's radio emission (Gurnett *et al.*, 2002). During the Cassini mission, work on the upper atmosphere of the planet can be tied into the *in situ* magnetospheric and solar wind measurements of the spacecraft. That will enable us to test the empirical relationships developed by Cowley and others. The availability both of observational data and modelling results means that many of the questions of ion-neutral coupling and the dynamics that engenders in the upper atmosphere, which we have only touched on in this chapter, can be investigated in detail. These studies can lead to a situation where

we can understand all of the factors, involved in the atmospheric energy balance, that go into determining the high exospheric temperatures of the giant planets. It may also be that progress can be made in reconciling observed electron profiles and those produced by models.

Acknowledgements

Global circulation model calculations for Jupiter and Saturn referred to in this chapter were carried out using the Miracle High Performance Computer Suite, which is part of the HiPerSPACE Centre at UCL, and funded by the UK Particle Physics and Astronomy Research Council. PPARC is also thanked for supporting the authors in various ways. Miller was a Visiting Astronomer at the IRTF, which is operated for NASA by the Institute for Astronomy, University of Hawaii.

References

Abel, B. and Thorne, R.M.: 2003, 'Relativistic charged particle precipitation into Jupiter's sub-auroral atmosphere', *Icarus* **166**, 311–319.

Achilleos, N., Miller, S., Tennyson, J., Aylward, A.D., Mueller-Wodarg, I., and Rees, D.: 1998, 'JIM: a time-dependent, three-dimensional model of Jupiter's thermosphere and ioniosphere', *J. Geophys. Res.* **103**, 20089–20112.

Atreya, S.K.: 1986, *The Atmosphere and Ionospheres of the Outer Planets and Their Satellites*, Springer Verlag, New York.

Ballester, G.E., and 21 other colleagues: 1998, 'Time-resolved observations of Jupiter's far ultraviolet auroras', *Science* **274**, 409–413.

Baron, R., Joseph, R.D., Owen, T., Tennyson, J., Miller, S., and Ballester, G.E.: 1991, 'Imaging Jupiter's aurorae from H_3^+ emissions in the 3–4 mm band', *Nature* **353**, 539–542.

Bhardwaj, A. and Gladstone, G.R.: 2000, 'Auroral emissions of the giant planets', *Rev. Geophys.* **38**, 295–353.

Broadfoot, A.L., and 18 others: 1986, 'Ultraviolet spectrometer observations of Uranus', *Science* **233**, 74–79.

Clarke, J.T., Caldwell, J., Skinner, T., and Yelle, R.: 1987, 'The aurora and airglow of Jupiter', *in* M.J.S. Belton, R.A. West, and J. Rahe (eds.), *Time Variable Phenomena in the Jovian System* NASA, Washington, pp. 211–228.

Clarke, J.T., and 10 co-workers: 1998, 'Hubble Space Telescope imaging of Jupiter's UV aurora during the Galileo orbiter mission', *J. Geophys. Res.* **103**, 20217–20236.

Clarke, J.T., and 11 co-workers: 2002, 'Ultraviolet emissions from the magnetic footprints of Io, Ganymede and Europa on Jupiter', *Nature* **415**, 997–1000.

Connerney, J.E.P., Baron, R., Satoh, T., and Owen, T.: 1993, 'Images of excited H_3^+ at the foot of the Io flux tube in Jupiter's atmosphere', *Science* **262**, 1035–1038.

Cowley, S.W.H. and Bunce, E.J.: 2001, 'Origin of the main auroral oval in Jupiter's coupled magnetosphere-ionosphere system', *Planet. Space Sci.* **49**, 1067–1088.

Cowley, S.W.H., Bunce, E.J., Stallard, T.S., and Miller, S.: 2003, 'Jupiter's polar ionospheric flows: theoretical interpretation', *Geophys. Res. Lett.* **30**, 1220.

Cowley, S.W.H., Bunce, E.J., and Prangé, R.: 2004, 'Saturn's polar ionospheric flows and their relation to the main auroral oval', *Ann. Geophysicae* **22**, 1379.

Drossart, P., Bézard, B., Atreya, S.K., Bishop, J., and Waite, J.H., Jr., and Boice, D.: 1993, 'Thermal profiles in the auroral regions of Jupiter', *J. Geophys. Res.* **98**, 18803–18810.

Dungey, J.W.: 1961, 'The interplanetary magnetic field and auroral zones', *Phys. Rev. Lett.* **6**, 47.

Feldman, P.D., McGrath, M.A., Moos, H.W., Durrance, S.T., Strobel, D.F., and Davidson, A.F.: 1993, 'The spectrum of the jovian dayglow observed at a 3A resolution with the Hopkins Ultraviolet Telescope', *Astrophys. J.* **406**, 279–284.

Gérard, J.-C., Dols, V., Grodent, D., Waite, J.H., Jr., and Prangé, R.: 1995, 'Simultaneous observations of the saturnian aurora and polar haze with the HST/FOC', *Geophys. Res. Lett.* **22**, 2685–2688.

Grodent, D., Waite, J.H., Jr., and Gérard, J.-C.: 2001, 'A self-consistent model of the jovian auroral thermal structure', *J. Geophys. Res.* **106**, 12933–12952.

Grodent, D., Clarke, J.T., Kim, J., Waite, J.H., Jr., and Cowley, S.W.H.: 2003, 'Jupiter's main auroral oval observed with HST-STIS', *J. Geophys. Res.* **108**, 9921–9937.

Gurnett, D.A., and 16 co-workers: 2002, 'Control of Jupiter's radio emission and aurorae by the solar wind', *Nature* **415**, 985–987.

Heaps, M.G.: 1975, 'The roles of particle precipitation and Joule heating in the energy balance of the jovian thermosphere', *Icarus* **29**, 273–281.

Herbert, F. and Sandel, B.R.: 1994, 'The uranian aurora and its relationship to the magnetosphere', *J. Geophys. Res.* **99**, 4143–4160.

Hickey, M.P., Walterscheid, R.L., and Schubert, G.: 2000, 'Gravity wave heating and cooling in Jupiter's thermosphere', *Icarus* **148**, 266–281.

Hill, T.W.: 1979, 'Inertial limit on corotation', *J. Geophys. Res.* **84**, 6554–6558.

Hill, T.W.: 2001, 'The jovian auroral oval', *J. Geophys. Res.* **106**, 8101–8107.

Hill, T.W. and Dessler, A.J.: 1991, 'Plasma motions in planetary magnetospheres', *Science* **252**, 410–415.

Huang, T.S. and Hill, T.W.: 1989, 'Corotation lag of the jovian atmosphere, ionosphere and magnetosphere', *J. Geophys. Res.* **94**, 3761–3765.

Isbell, J., Dessler, A.J., and Waite, J.H., Jr.: 1984, 'Magnetospheric energization by interaction between planetary spin and solar wind', *J. Geophys. Res.* **89**, 10716–10722.

Kim, Y.H., Fox, J.L., and Porter, H.S.: 1992, 'Densities and vibrational distribution of H_3^+ in the jovian auroral ionosphere', *J. Geophys. Res.* **97**, 6093–6101.

Kivelson, M.G., and 13 colleagues: 1997, 'Galileo at Jupiter: changing states of the magnetosphere and first look at Io and Ganymede', *Adv. Space Res.* **20**, 129.

Kivelson, M.G.: 2005, 'The current systems of the jovian magnetosphere and ionosphere and predictions for Saturn', this volume.

Lam, H.A., Miller, S., Joseph, R.D., Geballe, T.R., Trafton, L.M., Tennyson, J., and Ballester, G.E.: 1997a, 'Variation in the H_3^+ emission of Uranus', *Astrophys. J.* **474**, L73–L76.

Lam, H.A., Achilleos, N., Miller, S., Tennyson, J., Trafton, L.M., Geballe, T.R., and Ballester, G.E.: 1997b, 'A baseline spectroscopic study of the infrared auroras of Jupiter', *Icarus* **127**, 379–393.

Liu, W. and Dalgarno, A.: 1996, 'The ultraviolet spectrum of the jovian dayglow', *Astrophys. J.* **462**, 502–518.

Majeed, T. and McConnell, J.C.: 1991, 'The upper ionospheres of Jupiter and Saturn', *Planet. Space Sci.* **39**, 1715–1732.

Majeed, T., McConnell, J.C., and Yelle, R.V.: 1991, 'Vibrationally excited H_2 in the outer planets thermosphere: fluorescence in the Lyman and Werner bands', *Planet. Space Sci.* **39**, 1591–1605.

Majeed, T., Waite, J.H., Jr., Bougher, S.W., Yelle, R.V., Gladstone, G.R., McConnell, J.C., and Bhardwaj, A.: 2004a, 'The ionospheres-thermospheres of the giant planets', *Adv. Space Res.* **33**, 197–211.

Majeed, T., Waite, J.H., Bougher, S.W., and Gladstone, G.R.: 2004b, 'Jupiter thermosphere general circulation model I. Equatorial thermal structure', *J. Geophys. Res.*, submitted.

Matcheva, K.I. and Strobel, D.F.: 1999, 'Heating of Jupiter's thermosphere by dissipation of gravity waves due to molecular viscosity and heat conduction', *Icarus* **140**, 328–340.

Melin, H., Stallard, T., and Miller, S.: 2004, 'A new determination of Saturn's upper atmospheric temperature in the auroral/polar region', *Astrophys. J. Lett.*, in preparation.

Miller, S., Achilleos, N., Ballester, G.E., Lam, H.A., Tennyson, J., Geballe, T.R., and Trafton, L.M.: 1997, 'Mid-to-low latitude H_3^+ emission from Jupiter', *Icarus* **130**, 57–67.

Miller, S., and 10 other colleagues: 2000, 'The role of H_3^+ in planetary atmospheres', *Phil. Trans. Roy. Soc.* **358**, 2485–2502.

Millward, G., Miller, S., Stallard, T., Aylward, A.D., and Achilleos, N.: 2002, 'On the dynamics of the jovian ionosphere and thermosphere III: the modelling of auroral conductivity', *Icarus* **160**, 95–107.

Millward, G., Miller, S., Stallard, T., Achilleos, N., and Aywlard, A.D.: 2004, 'On the dynamics of the jovian ionosphere and thermosphere IV: ion-neutral coupling', *Icarus*, in press.

Moore, L., Mendillo, M., Mueller-Wodarg, I., and Murr, D.: 2004, 'Photochemical modelling of global variations and ring shadowing in Saturn's ionosphere', *Icarus*, submitted.

Moses, J.I. and Bass, S.F.: 2000, 'The effects of external material on the chemistry and structure of Saturn's ionosphere', *J. Geophys. Res.* **105**, 7013–7052.

Moses, J.I., Bézard, B., Lellouch, E., Gladstone, G.R., Feuchtgruber, H., and Allen, M.: 2000, 'Photochemistry of Saturn's atmosphere I. Hydrocarbon chemistry and comparisons with ISO observations', *Icarus* **143**, 244–298.

Mueller-Wodarg, I.C.F., Mendillo, M., Yelle, R.V., and Aylward, A.D.: 2004, 'A global circulation model of Saturn's thermosphere', *Icarus*, in press.

Pallier, L. and Prangé, R.: 2001, 'More about the structure of the high latitude jovian aurorae', *Planet. Space Sci.* **49**, 1159–1173.

Prangé, R., Rego, D., Pallier, L., Connerney, J.E.P., Zarka, P., and Quenniec, J.: 1998, 'Detailed study of FUV jovian auroral features with the post-COSTAR HST faint object camera', *J. Geophys. Res.* **103**, 20195–20215.

Pryor, W.R., Stewart, A.I.F., Simmons, K.E., Ajello, J.M., Tobiska, W.K., Clarke, J.T., and Gladstone, G.R.: 2001, 'Detection of rapdily varying H2 emissions in Jupiter's aurora from the Galileo orbiter', *Icarus* **151**, 314–317.

Rego, D., Achilleos, N., Stallard, T., Miller, S., Prangé, R., Dougherty, M., and Joseph, R.D.: 1999, 'Supersonic winds in Jupiter's aurorae', *Nature* **399**, 121–124.

Rego, D., Miller, S., Achilleos, N., Prangé, R., and Joseph, R.D.: 2000, 'Latitudinal profiles of the jovian IR emission of H_3^+ at 4 microns using the NASA Infrared Telescope Facility', *Icarus* **147**, 366–385.

Satoh, T., Connerney, J.E.P., and Baron, R.L.: 1996, 'Emission source model of Jupiter's H_3^+ aurorae: a generalised inverse analysis of images', *Icarus* **122**, 1–23.

Satoh, T. and Connerney, J.E.P.: 1999, 'Jupiter's H_3^+ emissions viewed in corrected jovimagnetic coordinates', *Icarus* **141**, 236–252.

Seiff, A., and 10 co-workers: 1998, 'Thermal structure of Jupiter's atmosphere near the edge of a 5-mm hot spot in the north equatorial belt', *J. Geophys. Res.* **103**, 22857–22890.

Smith, G.R., Shemansky, D.E., Holberg, J.B., Broadfoot, A.L., Sandel, B.R., and McConnell, J.C.: 1983, 'Saturn's upper atmosphere from the Voyager 2 EUV solar and stellar occultations', *J. Geophys. Res.* **88**, 8667–8678.

Smith, C., Aylward, A., Miller, S., and Mueller-Wodarg, I.C.F.: 2004, 'Polar heating in Saturn's thermosphere', *Ann. Geophysicae*, submitted.

Southwood, D.J. and Kivelson, M.G.: 2001, 'A new perspective on the influence of the solar wind on the jovian magnetosphere', *J. Geophys. Res.* **106**, 6123–6130.

Stallard, T., Miller, S., Millward, G., and Joseph, R.D.: 2001, 'On the dynamics of the jovian ionosphere and thermosphere I: the measurement of ion winds', *Icarus* **154**, 475–491.

Stallard, T.S., Miller, S., Cowley, S.W.H., and Bunce, E.J.: 2003, 'Jupiter's polar ionospheric flows: measured intensity and velocity variations poleward of the main auroral oval', *Geophys. Res. Lett.* **30**, 1221.

Stallard, T.S., Miller, S., Trafton, L.M., Geballe, T.R., and Joseph, R.D.: 2004, 'Ion winds in Saturn's southern auroral/polar region', *Icarus* **167**, 204–211.

Strobel, D.F. and Smith, G.R.: 1973, 'On the Temperature of the Jovian Thermosphere', *J. Atmos. Sci.* **30**, 718.

Strobel, D.F.: 2005, 'Photochemistry in outer solar system atmospheres', this volume.

Trafton, L.M., Miller, S., Geballe, T.R., Tennyson, J., and Ballester, G.E.: 1999, 'H_2 quadrupole and H_3^+ emission from Uranus: the uranian thermosphere, ionosphere and aurora', *Astrophys. J.* **524**, 1059–1083.

Trauger, J.T., and 16 co-workers: 1998, 'Saturn's hydrogen aurora: wide field planetary camera 2 imaging from Hubble Space Telescope', *J. Geophys. Res.* **103**, 20237–20244.

Vasavada, A.R., Bouchez, A.H., Ingersoll, A.P., Little, B., Anger, C.D., and the Galileo SSI Team: 1999, 'Jupiter's visible aurora and Io footprint', *J. Geophys. Res.* **104**, 27133–27142.

Vasyliunas, V.M.: 1983, 'Plasma distribution and flow', *in* A.J. Dessler (ed.), *Physics of the jovian magnetosphere*, Cambridge University Press, pp. 395–453.

Vincent, M.B., and 18 co-workers: 2000, 'Jupiter's polar regions in the ultraviolet as imaged by HST/WIFPC2: auroral aligned features and zonal motions', *Icarus* **143**, 205–222.

Waite, J.H., Jr., Cravens, T.E., Kozyra, J.U., Nagy, A.F., Atreya, S.K., and Chen, R.H.: 1983, 'Electron precipitation and related auronomy of the jovian thermosphere and ionosphere', *J. Geophys. Res.* **88**, 6143–6163.

Waite, J.H., Jr., Gladstone, G.R., Lewis, W.S., Drossart, P., Cravens, T.E., Maurelis, A.N., Mauk, B.H., and Miller, S.: 1997, 'Equatorial X-ray emissions: implications for Jupiter's high exospheric temperatures', *Science* **276**, 104–108.

Waite, J.H., Jr., and 10 co-workers: 2001, 'An auroral flare at Jupiter', *Nature* **410**, 787–789.

Waite, J.H., Jr. and Lummerzheim, D.: 2002, 'Comparison of auroral processes: Earth and Jupiter, *in* M. Mendillo, A. Nagy, and J.H. Waite (eds.), *Atmospheres in the Solar System*, AGU Geophysical Monograph **130**, 115–139.

Yelle, R.V. and Miller, S.: 2004, 'Jupiter's thermosphere and ionosphere *in* F. Bagenal, T.E. Dowling, and W.B. McKinnon (eds.), *Jupiter: The Planet, Satellites and Magnetosphere* Cambridge University Press.

Young, L.A., Yelle, R.V., Young, R.E., Seiff, A., and Kirk, D.B.: 1997, 'Gravity waves in Jupiter's thermosphere', *Science* **276**, 108–111.

Address for Offprints: Steve Miller, Atmospheric Physics Laboratory, Department of Physics and Astronomy, University College London, London WC1E 6BT, UK; ucapt0s@ucl.ac.uk